Published online 9 July 2021

Nucleic Acids Research, 2021, Vol. 49, No. 14 ***8277–8293***
https://doi.org/10.1093/nar/gkab599

Golgi-58K can re-localize to late endosomes upon cellular uptake of PS-ASOs and facilitates endosomal release of ASOs

Xue-Hai Liang [1,*], Joshua G. Nichols[1], Cheryl Li De Hoyos[1], Hong Sun[2], Lingdi Zhang[1] and Stanley T. Crooke [1]

[1]Core Antisense Research, Carlsbad, CA 92010, USA and [2]Antisense Drug Discovery, Ionis Pharmaceuticals, Inc., Carlsbad, CA 92010, USA

Received April 21, 2021; Revised June 21, 2021; Editorial Decision June 26, 2021; Accepted June 29, 2021

ABSTRACT

Phosphorothioate (PS) modified antisense oligonucleotide (ASO) drugs can trigger RNase H1 cleavage of cellular target RNAs to modulate gene expression. Internalized PS-ASOs must be released from membraned endosomal organelles, a rate limiting step that is not well understood. Recently we found that M6PR transport between Golgi and late endosomes facilitates productive release of PS-ASOs, raising the possibility that Golgi-mediated transport may play important roles in PS-ASO activity. Here we further evaluated the involvement of Golgi in PS-ASO activity by examining additional Golgi proteins. Reduction of certain Golgi proteins, including Golgi-58K, GCC1 and TGN46, decreased PS-ASO activity, without substantial effects on Golgi integrity. Upon PS-ASO cellular uptake, Golgi-58K was recruited to late endosomes where it colocalized with PS-ASOs. Reduction of Golgi-58K caused slower PS-ASO release from late endosomes, decreased GCC2 late endosome relocalization, and led to slower retrograde transport of M6PR from late endosomes to trans-Golgi. Late endosome relocalization of Golgi-58K requires Hsc70, and is most likely mediated by PS-ASO–protein interactions. Together, these results suggest a novel function of Golgi-58K in mediating Golgi-endosome transport and indicate that the Golgi apparatus plays an important role in endosomal release of PS-ASO, ensuring antisense activity.

INTRODUCTION

Antisense oligonucleotide (ASO) drugs hybridize with target RNAs and modulate gene expression by triggering different post-hybridization mechanisms (1–5). Gapmer ASOs that induce RNase H1-mediated target RNA degradation are normally designed with a ∼10-nucleotide (nt) central DNA portion flanked at both ends with 3–5 2′-modified nucleotides, such as 2′-methoxyl ethyl (MOE), constrained ethyl (cEt) or 2′-fluoro (F) modifications. In addition, commonly used gapmer ASOs are modified with phosphorothioate (PS) backbones that dramatically increase protein binding compared with phosphodiester (PO) backbone ASOs while also enhancing stability, distribution into tissues and cells, and pharmacological properties (6).

ASOs must enter cells and reach the target RNAs in cytosol and nucleus to elicit antisense activity (7). PS-ASOs enter cells primarily via the endocytic pathways and PS-ASO internalization mediated by cell-surface receptors tends to direct PS-ASOs to productive pathways, through which PS-ASOs can act on target RNAs (8–12). Internalized PS-ASOs transport quickly into early endosomes (EEs) and late endosomes (LE) within 10–50 min, and finally localize to lysosomes (Figure 1) (13). However, PS-ASO release from endocytic organelles is a relatively slow process since PS-ASO activity is observed only after 6–8 hours of PS-ASO incubation without transfection reagent (referred to here as free uptake) (14). It appears that LEs, or multivesicular bodies (MVBs) are major sites for productive PS-ASO release (8,11,15–17). Only a small portion of internalized PS-ASOs are released from the membraned endocytic organelles (18), and endosomal release appears to be a limiting factor of PS-ASO antisense activity. Thus, a better understanding of PS-ASO release mechanisms will facilitate the design of PS-ASOs to improve drug performance.

Previously, we found that some proteins are recruited to LEs in cells incubated with PS-ASOs by free uptake and contribute to ASO activity (19). For example, a lipid interacting protein, ANXA2, is enriched in LEs after PS-ASO cellular uptake and enhances PS-ASO activity by facilitating PS-ASO transport from EEs to LEs and endosomal release (Figure 1) (13,19). PS-ASOs can localize in intralumenal vesicles (ILVs) inside LE-limiting membranes, and some proteins can also colocalize with PS-ASOs at ILVs

*To whom correspondence should be addressed. Tel: +1 760 603 3816; Fax: +1 760 603 2600; Email: Lliang@ionisph.com

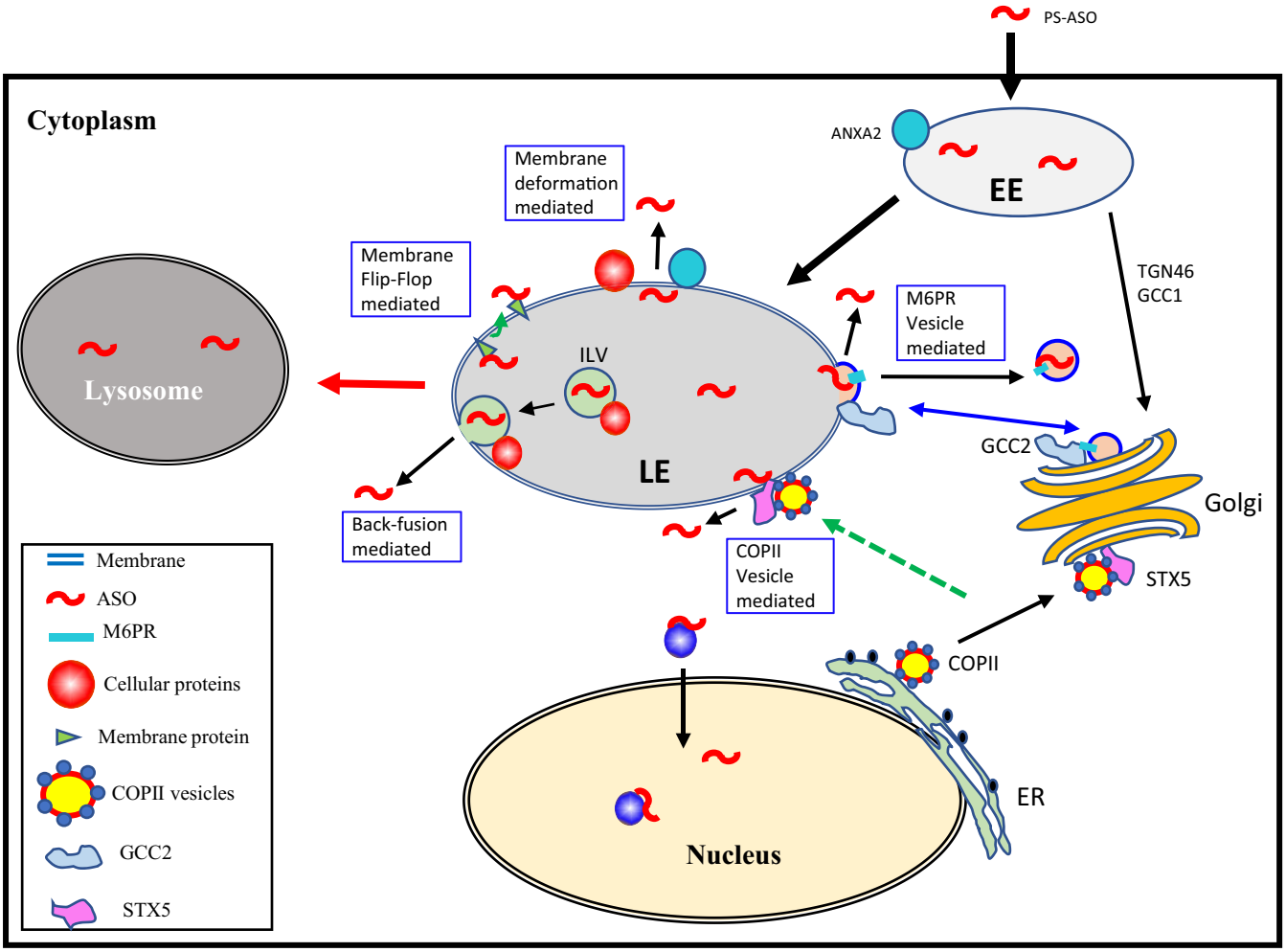

Figure 1. Schematic representation of intracellular trafficking and endosomal release pathways of PS-ASOs. Internalized PS-ASOs quickly localize to EEs, and traffic through LEs, as indicated by thick black lines. PS-ASOs localization to lysosomes (marked with a red arrow) is considered to be non-productive. LEs appear to be the major site of productive PS-ASO release. Some cellular proteins, including ANXA2, can relocalize to LEs, either on LE limiting membranes or at ILVs inside LEs, and facilitate PS-ASO release. Several release mechanisms have been proposed, including membrane deformation facilitated by protein interaction with LE membranes, ILV-mediated back-fusion process, and vesicle-mediated release. STX5-mediated COPII vesicles that normally traffic between ER and Golgi, and GCC2-mediated M6PR vesicles that normally traffic between LE and TGN (blue line), can relocate to LEs upon PS-ASO cellular uptake and facilitate ASO release.

(15,17,20). It has been proposed that endosomal release of PS-ASOs occurs through multiple pathways that co-exist and that may act in parallel (Figure 1) (8,11,14,20). For instance, membrane flip-flop may cause PS-ASOs inside LEs to be exposed to the cytosol (21); interactions of proteins with LE membranes may trigger membrane deformation and PS-ASO leakage (13); and PS-ASO release may also occur when ILV membranes fuse with the limiting membranes of LEs through a back-fusion process (17). Due to the existence of multiple PS-ASO release pathways, blocking a particular pathway normally causes only modest defects in PS-ASO release and activity.

More recently, we demonstrated that cellular vesicle-mediated transport pathways are also involved in PS-ASO release from endosomes (Figure 1). Coat protein complex II (COPII) vesicles, which normally transport membrane and secreted proteins from the ER to the Golgi (22), can be recruited to LEs upon PS-ASO uptake and facilitate PS-ASO release (14). This process is mediated by Golgi related proteins P115 and STX5. STX5 is recruited to LEs upon PS-ASO cellular uptake, likely mediated by PS-ASO-protein interactions (14). In addition, Mannose 6-phosphate receptor (M6PR), which shuttles in vesicles between trans-Golgi network (TGN) and LEs to transport newly synthesized lysozymes (23), is also involved in PS-ASO release independent of the COPII pathway (20). M6PR shuttling requires a Golgi protein GCC2, which tethers incoming M6PR vesicles to the membranes of TGN (24). Upon PS-ASO cellular uptake, GCC2 is recruited to LEs (20), in a Hsc70 protein dependent manner (25). Interestingly, Hsc70 was found to be involved in M6PR vesicle budding from LEs (25).

Given the important roles of Golgi in material sorting and transport between ER-Golgi-Endosomes, and the observations that some Golgi related proteins, for example, STX5, GCC2 and M6PR, are involved in PS-ASO intracellular trafficking and endosomal release, it is very likely that the Golgi apparatus plays an important role in modulating PS-ASO activity. To further understand the role of the

Golgi in PS-ASO activity and endosomal release, we characterized the potential involvement of six additional Golgi proteins in modulating PS-ASO activity. We found that reduction of Golgi-58K, Mannosidase II (Man2A1), TGN46, and GCC1 also decreased PS-ASO activity. Golgi-58K is recruited to LEs upon PS-ASO incubation, and can colocalize with PS-ASOs at ILVs and on the LE membranes. Golgi-58K relocalization to LEs requires Hsc70, and most likely involves protein-ASO interactions. Importantly, Golgi-58K affects GCC2 relocalization to LEs upon PS-ASO incubation, and is involved in M6PR shuttling, suggesting a novel biological function of Golgi-58K. Thus, this study further unveils the importance of the Golgi, especially TGN – LE shuttling pathways, in endosomal release of PS-ASOs. In addition, our study also identified a functional cluster of proteins involved in M6PR shuttling-mediated PS-ASO release from LEs.

MATERIALS AND METHODS

Materials

ASOs (Supplementary Table S1), siRNAs and primer probes (Supplementary Table S2), and antibodies (Supplementary Table S3) are listed in Supplementary Materials.

Cell culture and treatment with siRNAs or ASOs

HeLa, A431, HEK293, HepG2, MHT or SVGA cells expressing GFP-Rab7 (a kind gift from Dr Tomas Kirchhausen's lab) were cultured in Dulbecco's modified Eagle's medium supplemented with 10% Fetal Bovine Serum (FBS), 0.1 μg/ml streptomycin and 100 units/ml penicillin. Cells were seeded at ∼70% confluency and grown for 16 h before transfection. siRNAs were transfected for 48–72 h using 6 μg/ml Lipofectamine RNAiMax (Life Technologies), at 3–6 nM final siRNA concentration, as described previously (26). For PS-ASO activity assays under free uptake, siRNA treated cells were re-seeded into 96-well plates at ∼75% confluency. After 8 h, PS-ASOs were added to the medium without transfection reagent and cells continued to grow overnight before RNA preparation the next day. PS-ASO activity assay under transfection was performed as described previously (27). Briefly, cells treated with siRNA for 48 h were reseeded in 96-well plates, incubated overnight, followed by PS-ASO transfection for 4 h using 4 μg/ml Lipofectamine 2000 (Life Technologies) before RNA preparation.

RNA preparation and qRT-PCR analysis

Total RNA was prepared using RNeasy mini kit (Qiagen), based on the manufacturer's instructions. Quantitative real-time polymerase chain reaction (qRT-PCR) was performed in triplicate using StepOne Real-Time PCR system and TaqMan primer probe sets with Ag-PathID™ One-step RT-PCR kit (Applied Biosystems). qRT-PCR in 20 μl reactions was performed using the following program: 48°C for 10 min, 94°C for 10 min and 40 cycles of 20 s each at 94 and 60°C. The qRT-PCR results were quantified using StepOne Software V2.3, calculated and plotted using Excel. Target RNA levels were normalized to the levels of total RNA measured using SYBR Green (Life Technologies). Statistical analysis was performed using Prism, with *F*-test for curve comparison based on non-linear regression (dose–response curves) for XY analyses, using equation 'log(agonist) versus normalized response –variable slop'. The Y axis (relative mRNA level) was directly used as the normalized response.

Western analysis

Cells were collected using trypsin and washed once with ice-cold 1× PBS. Cell lysate was prepared using RIPA buffer (ThermoFisher) and cleared by centrifugation at 10 000 × g for 10 min at 4°C. Proteins (20–40 μg/lane) were separated by 4–12% SDS-PAGE, transferred to membranes using iBlot transfer system (Life Technologies). Proteins were detected with specific antibodies, and visualized using ECL, as described elsewhere.

Immunofluorescence staining

Unless specified in figure legends, cells grown in glass-bottom dishes were incubated with 2 μM Cy3-labeled PS-ASOs for 16–24 h. Cells were then washed with 1× PBS, fixed with 4% paraformaldehyde for 0.5–1 h, and permeabilized with 0.1% Triton in 1× PBS for 4 min at room temperature. After incubation at room temperature for 30 min with block buffer (1 mg/ml BSA in 1× PBS), cells were incubated with primary antibodies (1:100–1:300) in block buffer for 4 h, washed three times (5 min each) using wash buffer (0.1% NP-40 in 1× PBS), and incubated for 1 h with fluorophore-conjugated secondary antibodies (1:200). After washing three times, cells were mounted with Antifade reagent containing DAPI (Life Technologies), and images were taken using confocal microscope (Olympus FV-1000) and processed with FV-10 ASW 3.0 Viewer software (Olympus). Z-stacks were generated from images taken at 0.1 μm depth per section, and 3D movies were generated using FV-10 ASW-3.0 viewer. For early time staining after PS-ASO incubation (20 min), cells were washed three times with acidic buffer (0.1M acetic acid, 500 mM NaCl) and one time with 1× PBS, to remove cell surface associated PS-ASOs before fixation. Quantification of co-localization events was performed manually from ∼20 cells, by counting overlapping foci of which images from both channels have clearly defined boundary without saturation. Statistics analysis was performed based on unpaired *t*-test using prism.

Live cell imaging and measurement of PS-ASO signal in live cells

For the co-movement of PS-ASO foci in LEs, SVGA cells expressing GFP-Rab7 were incubated with 2 μM Cy3-PS-ASO for 16 h. Medium was then changed to prewarmed Opti-MEM medium (Life Technologies). LE movement was recorded at highest speed using confocal microscopy (Olympus FV-1000), at 37°C in an environmental chamber. Live cell movie was then processed using FV-10 ASW-3.0 software.

For measurement of PS-ASO signal in live cells, SVGA cells pretreated with siRNAs for 48 h were reseeded in glass-

bottom dishes, incubated at 37°C for 8 h, and 3 μM Cy3-PS-ASO was added to the medium. After 16 h, cells were washed with PBS, and pre-warmed OPTI medium (Invitrogen) was added to the dishes. Live cell movies were taken using confocal microscope in an environmental chamber at 37°C, with GFP and Cy3 channels for RAB7 and PS-ASO, respectively, for 100 rounds of free run (highest speed). Cy3 signal were measured using FV-10 ASW-3.0 software. Since LEs can move in live cells, for endosomal ASO signal measurement, the perinuclear areas without LE moving in or out of the selected areas over time were quantified. The signal intensity in a selected area at a given time point was calculated as the percentage of the signal intensity of the same area at time point 0 (start time). The relative levels of ASOs were calculated from ∼15 cells, and the means and standard deviations were plotted.

M6PR-CI antibody transport

Control, or Golgi-58K reduced HeLa cells were incubated with 5 μg/ml antibody against M6PR-CI (ab2733, from Abcam) in cold Opti-MEM medium on ice for 15 min. Cells were then shifted to 37°C incubator and incubated for either 75 min or 2 h. Cells were subsequently washed with PBS, fixed with 4% paraformaldehyde, permeabilized and blocked using 1 mg/ml BSA. HeLa cells were stained for Rab7 using a rabbit-raised primary antibody. Anti-Rab7 antibody and internalized anti-M6PR-CI antibody were detected with corresponding anti-rabbit and anti-mouse secondary antibodies conjugated with AF647 and AF488, respectively.

Colocalization analyses of confocal images

Images of the same groups to be compared were taken under the same settings without saturation. Colocalization analyses between PS-ASOs and a given protein were performed using JACoP plugin for ImageJ-Fiji (28,29). Pearson's correlation coefficient analysis was chosen to reduce the influence of background signals from different channels. Colocalization coefficient was determined from four images of each group, with constant settings for minimum and maximum threshold values. To determine random colocalization, one channel was rotated 90°C and Pearson's coefficient was measured. PS-ASO induced protein–protein colocalization at LEs was analyzed with the Coloc 2 function of ImageJ-Fiji. PS-ASO channel was used to set up region of interest (ROI) to determine PS-ASO induced LE colocalization of different proteins, and the ROIs were applied to the AF488 channel, and the colocalization of the AF488-stained proteins in the ROIs with the proteins stained with AF647 channel was analyzed. Mean values of Pearson's coefficient and standard deviations were calculated based on the results from four images of each group.

PS-ASO uptake analysis

HeLa cells treated with different siRNAs for 48 h were reseeded into 96-well plates, incubated in a 37°C incubator overnight, and Cy3-labeled PS-ASO 446654 was added at different concentration in triplicate to the medium. After 4 h, cells were washed three times with 1× PBS, and Cy3 signals were measured in triplicate per group using a Tecan microplate reader. Average values and standard deviations were plotted.

Affinity selection

Affinity selection using biotinylated PS-ASOs was performed as described previously (27). Briefly, neutravidin beads precoated with biotin-conjugated PS-ASO 386652 were incubated for 2 h with whole cell lysate prepared without, or with 5 mM of either $MgCl_2$ or $CaCl_2$. After incubation, beads were washed five times, and proteins were eluted and analyzed by western analysis. For ASO-Golgi-58K interaction, biotin-conjugated ASOs, either a phosphodiester (PO) backbone ASO modified with 2′-*O*-methyl (XL1149) or a PS backbone ASO modified with 2′-MOE at both ends (ASO 386652), were incubated with neutravidin beads, and blocked with block buffer (1 mg/ml BSA in PBS) for 30 min at room temperature. After washing with W-200 buffer (50 mM Tris–HCl (pH 7.5), 200 mM KCl, 5 mM ethylenediaminetetraacetic acid (EDTA), 0.1% NP-40, 0.05% sodium dodecyl sulphate (SDS)), the beads were incubated with 0.5 μg recombinant human Golgi-58K protein (Origen) mixed with 50 μg BSA for 2 h at 4°C. After washing five times with W-200 buffer, beads-bound proteins were analyzed by SDS-PAGE, and Golgi-58K protein was detected by western blotting using a Golgi-58K specific antibody (Abcam, ab19072).

RESULTS

Golgi-58K can re-localize to LEs upon PS-ASO free uptake

Previously we found that Golgi related proteins STX5 and GCC2 can be recruited to LEs upon PS-ASO cellular uptake and facilitate PS-ASO release, through COPII and M6PR pathways, respectively (Figures 1, 14 and 20). To further examine the potential roles of Golgi apparatus in PS-ASO trafficking and activity, HeLa cells were incubated with a Cy3-labeled, 2′-MOE modified gapmer PS-ASO by free uptake. Next, the localization pattern of a Golgi marker protein, Golgi-58K, and a LE/Lysosome marker protein, LAMP1, was determined by immunofluorescence staining. It has been reported that Golgi-58K [Formiminotransferase Cyclodeaminase (FTCD)] has dual metabolic functions and may also be involved in linking Golgi and vimentin filaments (30,31). In control cells without PS-ASO incubation, Golgi-58K protein stained the Golgi region, as expected, and no co-localization between Golgi-58K and LAMP1 was detected (Figure 2A). Surprisingly, upon cellular uptake of PS-ASOs, Golgi-58K appeared as dot-like structures scattered in the cytoplasm (Figure 2B). Such dot like-structures colocalized with PS-ASOs, and many such foci also colocalize with LAMP1, indicating that Golgi-58K may be recruited to LEs, as is the case for GCC2 and STX5 proteins (14,20). To further confirm the LE localization of Golgi-58K upon PS-ASO uptake, Cy3-labeled PS-ASO was incubated with GFP-Rab7 expressing SVGA cells (Figure 2C). Immunofluorescence staining result showed that Golgi-58K indeed colocalized with PS-ASO and with GFP-Rab7, a LE marker protein. The colocalization of

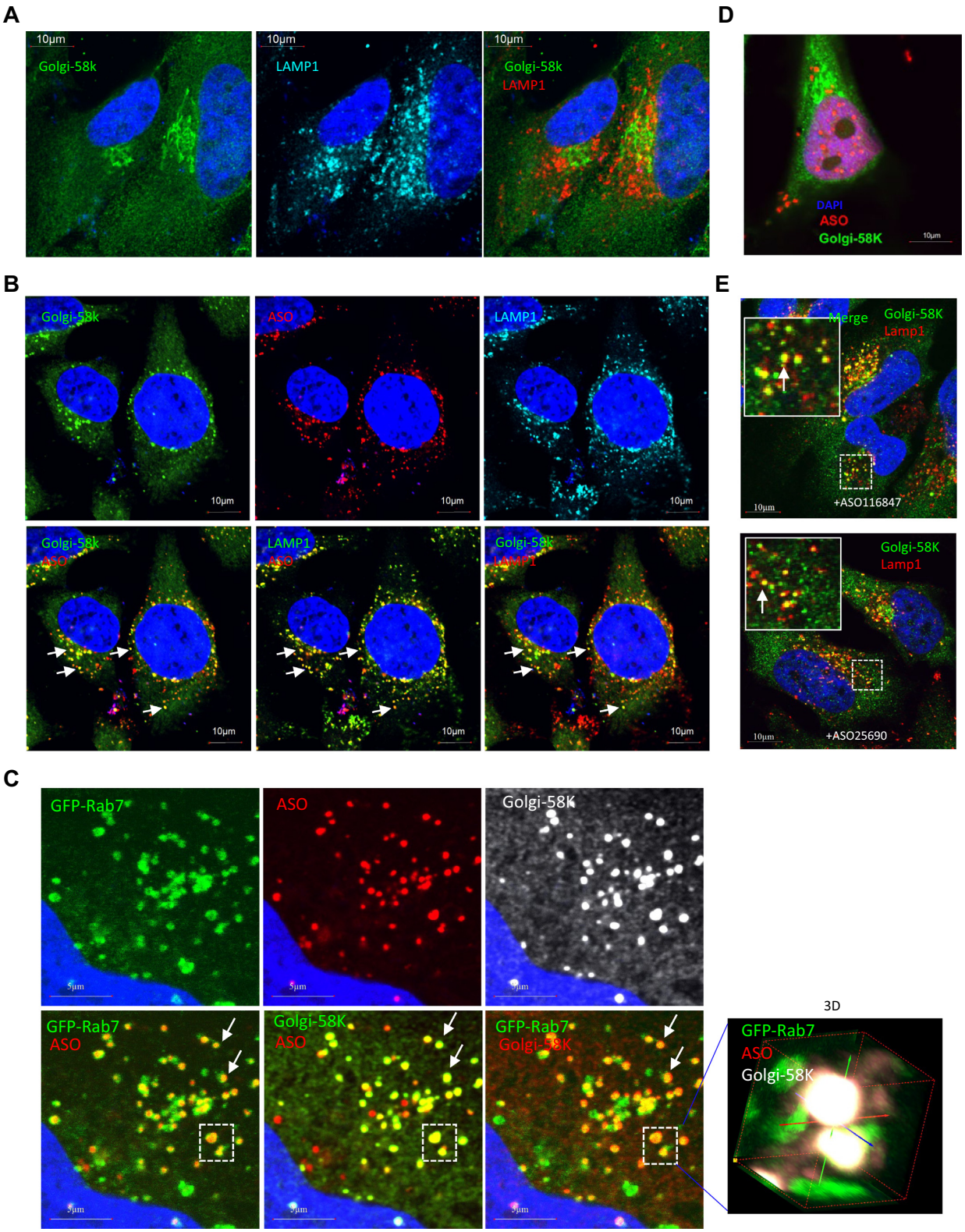

Figure 2. Golgi-58K can relocate to LEs upon PS-ASO cellular uptake. (**A**) Immunofluorescence staining of Golgi-58K and LAMP1 in HeLa cells. (**B**) Immunofluorescence staining of Golgi-58K and LAMP1 in HeLa cells incubated for 24 h with 2 μM Cy3-labeled PS-ASO 446654. PS-ASO/Golgi-58K colocalizations at LEs are exemplified by arrows. (**C**) Immunofluorescence staining of Golgi-58K in SVGA cells expression GFP-Rab7 that were incubated with 2 μM Cy3-labeled PS-ASO 446654 for overnight. Z-section imaging was performed for two LEs (boxed) and the 3D image is shown in right panel. (**D**) Immunofluorescence staining of Golgi-58K in HeLa cells transfected with 50 nM Cy3-labeled PS-ASO for 16 h. (**E**) Immunofluorescence staining of Golgi-58K and LAMP1 in HeLa cells incubated with 2 μM unlabeled PS-ASOs 116847 or 25690 for 16 h. Scale bars, 10 μm or 5 μm, as indicated in figures.

Golgi-58K with PS-ASO at LEs was also confirmed by 3D-imaging (Figure 2C, right panel).

Although the choice of antibody may cause non-specific staining and PS-ASO localization may be affected by the labeling dyes or fixation, several lines of evidence suggest that PS-ASO-Golgi-58K colocalization was not due to staining artifact. The Golgi-58K antibody appears specific, as treatment with Golgi-58K siRNA reduced the staining signal (Supplementary Figure S1A, B). In addition, colocalization between PS-ASO and Golgi-58K was also confirmed using a different Golgi-58K antibody (Supplementary Figure S1C). The colocalization between Golgi-58K and PS-ASO appears not to be due to potential channel leakage, as a Cy5-labeled PS-ASO could colocalize with Golgi-58K when the protein was stained using a FITC-conjugated secondary antibody (Supplementary Figure S1D). On the other hand, no Golgi-58K was found to colocalize with PS-ASOs upon transfection (Figure 2D), an approach largely bypasses the normal endocytic trafficking and release process and delivers PS-ASOs mainly to the cytosol and the nucleus (27). Moreover, the LE localization of Golgi-58K was not due to the presence of the Cy3 dye, as the unlabeled PS-ASO counterpart that has the same sequence and chemistry as the Cy3-labeled PS-ASO also caused Golgi-58K relocalization to LEs as marked with LAMP1 (Figure 2E). Similar LE relocalization of Golgi-58K was observed with another unlabeled PS-ASO (ASO25690) that is used in subsequent studies for PS-ASO activity assays (see below), suggesting that the relocalization of Golgi-58K to LE is not unique to one PS-ASO sequence.

Consistently, two additional Cy3-labeled PS-ASOs were tested, and all these PS-ASOs showed colocalization with Golgi-58K in dot-like cytoplasmic foci (Supplementary Figure S2A). In addition to the 2′-MOE modified, Cy3-labeled 5–10–5 PS-ASOs as used above, Golgi-58K colocalized with 5–10–5 PS-ASOs containing 2′-cEt or 2′-F modifications, and with 3–10–3 PS-ASOs modified with 2′-cEt (Supplementary Figure S2B). Furthermore, such colocalizations were observed in human A431, HEK293 and HepG2 cells, as well as mouse MHT cells (Supplementary Figure S3), suggesting a general phenomenon in different cell types and species. Together, these results indicate that Golgi-58K can be recruited to LEs in different cell types upon PS-ASO cellular uptake, independent of the PS-ASO sequences or 2′ modifications.

Previously, we have shown that some Golgi proteins, such as GM130 and STX16, are not recruited to LEs upon PS-ASO incubation (14,20). Consistent with these earlier observations that not all tested Golgi proteins relocalize to LEs, we found here that another Golgi marker protein, Mannosidase II (Man2A1) (32), also did not colocalize with PS-ASOs at LEs upon PS-ASO uptake (Supplementary Figure S4), further indicating that not all Golgi proteins behave similarly and that only certain proteins, including Golgi-58K, could be recruited to LEs upon PS-ASO uptake. These results also suggest that cellular uptake of PS-ASOs did not disrupt the integrity of Golgi structures, consistent with our previous observations that ASO cellular uptake does not affect Golgi function as indicated by the unaltered levels of secreted glycoproteins (14).

Reduction of Golgi-58K decreased PS-ASO activity in different cell types upon free uptake

As LEs are the major sites for productive PS-ASO release (1,8,11), the recruitment of Golgi-58K protein to LEs upon PS-ASO incubation may affect PS-ASO activity, like other cellular proteins recruited to LEs (13,14,19,20). To evaluate this possibility, expression of Golgi-58K was reduced in HeLa cells using siRNAs (Figure 3A). Detection of Golgi-58k protein levels by western failed, after attempting with several different antibodies (data not shown), likely due to the low levels of this protein in these cells. However, reduced Golgi-58K protein levels were detected by immunofluorescence staining (Supplementary Figure S1B and Supplementary Figure S5A). As a control, TMED9, another Golgi trans-membrane protein involved in COP I/II trafficking between ER and Golgi (33), was also reduced by siRNA treatment (Figure 3A, Supplementary Figure S5B).

Cells were incubated for 18 h with PS-ASOs targeting two different RNAs, the cytoplasmic *Drosha* mRNA and the nuclear Malat1 RNA and the cells were allowed to ingest PS-ASOs by free uptake. We note that under the experimental conditions even with high PS-ASO concentrations, no cell morphological changes or growth defects were observed (data not shown). The PS-ASO activity was determined by qRT-PCR quantification for the levels of the target RNAs. Reduced PS-ASO activities in degrading the target RNAs were observed in cells treated with the Golgi-58K siRNA, and not with the TMED9 siRNA, as compared with that in luciferase siRNA treated control cells (Figure 3B). Reduction of Golgi-58K also decreased the activities of two additional PS-ASOs targeting *NCL* and *PTEN* mRNAs, respectively (Supplementary Figure S6A). In addition, depletion of Golgi-58K using a different siRNA similarly decreased PS-ASO activity in HeLa cells (Supplementary Figure S6B, C). Moreover, reduced PS-ASO activity was also detected in A431 cells treated with Golgi-58K siRNA (Supplementary Figure S6D, E), suggesting that the observed phenotype is not unique to a single cell type. Together, these results indicate that Golgi-58K facilitates PS-ASO activity in cells.

When PS-ASOs were delivered by transfection, an approach that largely bypasses normal internalization and endosomal release process and robustly delivers ASOs to cytosol and nucleus, PS-ASO activity was not decreased upon Golgi-58K reduction (Figure 3C). These results suggest that Golgi-58K is not required for PS-ASO activity after release of PS-ASOs from endosomal organelles. Consistently, reduction of Golgi-58K did not reduce the levels of RNase H1 protein (Supplementary Figure S7), the enzyme responsible for gapmer PS-ASO-mediated degradation of target RNAs (34), or a few other proteins known to be involved in PS-ASO activity (19). Together, these results suggest that Golgi-58K is most likely involved in PS-ASO endocytic trafficking and/or endosomal release process(s), through which it affects PS-ASO activity.

Reduction of certain Golgi localized proteins can also decrease PS-ASO activity

Since reduction of TMED9 and GM130 did not affect PS-ASO activity, as shown above and previously (20), yet reduction of Golgi-58K, STX5 and GCC2 proteins decreased

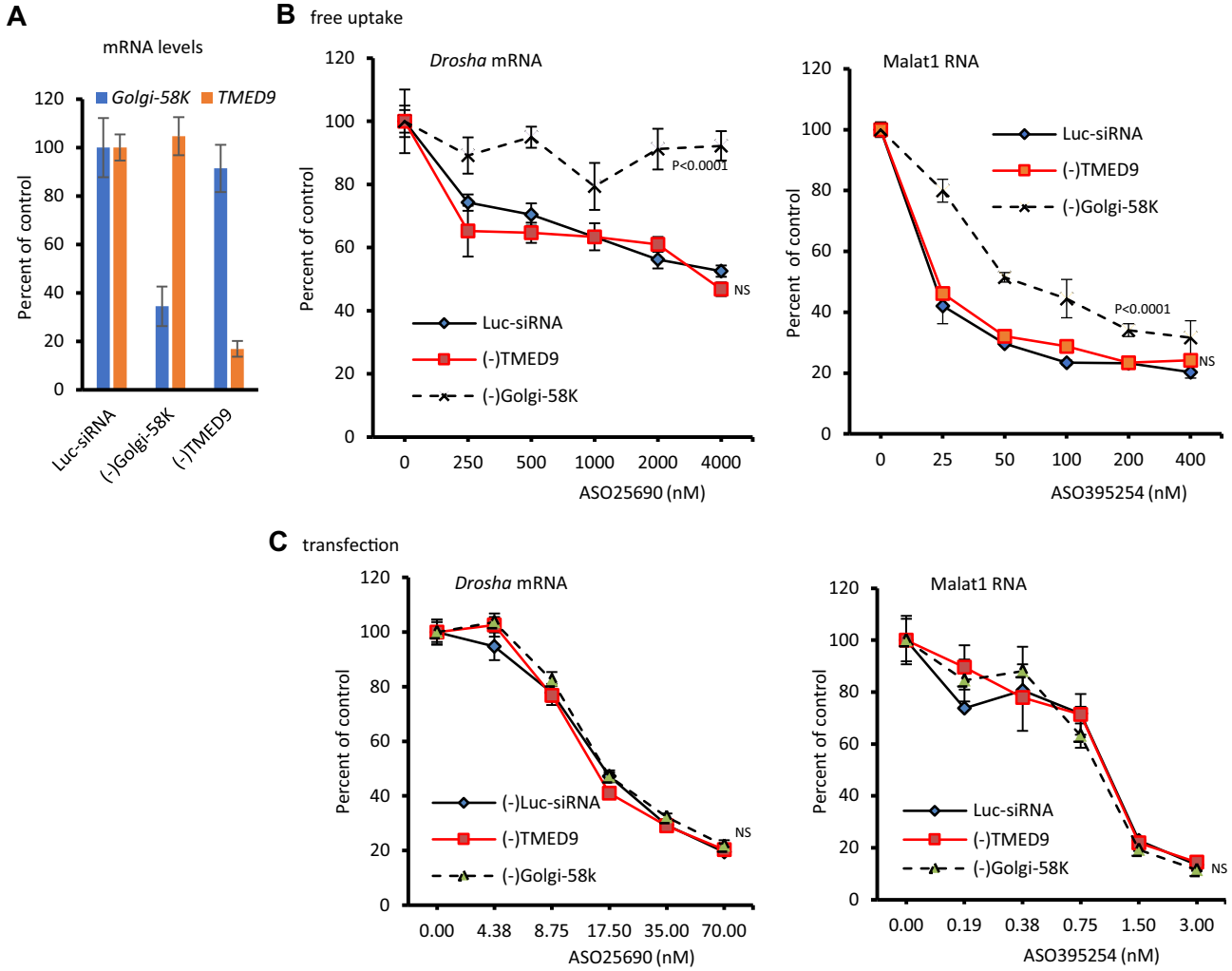

Figure 3. Reduction of Golgi-58K decreased PS-ASO activity upon free uptake. (**A**) qRT-PCR quantification of *Golgi-58K* and *TMED9* mRNAs in HeLa cells transfected with different siRNAs for 48 h. (**B**) qRT-PCR quantification of *Drosha* (left panel) or *Malat1* (right panel) RNA levels in HeLa cells pre-treated with different siRNAs for 48 h, followed by incubation for 24 h with different concentrations of corresponding PS-ASOs targeting *Drosha* and *Malat1* RNAs. (**C**) qRT-PCR quantification of *Drosha* (left panel) or *Malat1* (right panel) RNA levels in HeLa cells pre-treated with different siRNAs for 48 h, followed by transfection for 4 h with different concentrations of corresponding PS-ASOs targeting *Drosha* and *Malat1* RNAs. Error bars represent standard deviations from three independent experiments. *P* values were calculated based on *F*-test using Prism. NS, not significant.

PS-ASO activity, it appears that not all Golgi localized proteins are involved in PS-ASO trafficking, or action. To further explore the involvement of Golgi in PS-ASO activity, several additional Golgi proteins were reduced by siRNA treatment. These include TMED10 that belongs to the P24 protein family like TMED9 and is also involved in COP I/II shuttling between ER and Golgi (33); GCC1, a peripheral membrane protein involved in TGN46 (TGN38) retrograde transport from EE to TGN (35,36); and TGN46 itself that traffics between TGN and EE and may mediates the formation of post-TGN vesicles (37,38). In addition, another Golgi protein, alpha-Mannosidase II (Man2A1), that is involved in the protein glycosylation process (39), was also evaluated.

Under the experimental conditions, reduction of TMED10 by siRNA treatment did not affect PS-ASO activity (Supplementary Figure S8A,B), similarly to TMED9, although these proteins are required for ER-Golgi vesicular trafficking (33). However, reduction of Man2A1, GCC1, or TGN46 caused modest reduction in PS-ASO activity upon free uptake (Supplementary Figure S8C–H). These experiments were repeated three times and similar results were observed (data not shown), suggesting that the reduced PS-ASO activities upon depletion of these proteins are reproducible, though modest. Similar effects on PS-ASO activity were observed when different siRNAs targeting these genes were used (data not shown). On the other hand, no loss of PS-ASO activity was observed in cells depleted of these proteins by siRNA treatment when PS-ASOs were transfected (Supplementary Figure S8I). These observations suggest that these proteins may affect PS-ASO activity at steps before ASOs are released to cytosol and nucleus, likely at endosomal trafficking and/or release processes.

Currently it is unclear how these Golgi proteins contribute to PS-ASO activity. Although GCC1 can bind PS-

ASOs as determined by affinity selection (Supplementary Figure S9A), no substantial colocalization of GCC1 with PS-ASOs was detected upon free uptake (Supplementary Figure S9B), unlike the case of Golgi-58K or GCC2. In addition, reduction of GCC1 and TGN46 did not alter the structure of Golgi-58K stained Golgi apparatus, consistent with previous observations (35), whereas reduction of Man2A1 led to modestly scattered Golgi (Supplementary Figure S10A). Reduction of these three proteins also did not substantially alter colocalization of Golgi-58K with PS-ASOs (Supplementary Figure S10B, C). However, TGN46 could be detected in EEs (Supplementary Figure S11A), in agreement with previous reports (35). Upon brief PS-ASO incubation (20 min) to allow PS-ASOs to enter EEs, TGN46 colocalized with PS-ASOs in EEs (Supplementary Figure S11B), in agreement with previous findings that TGN46 can traffic from EE to TGN (35). In the absence of PS-ASOs, TGN46 was not detected at LEs marked with Rab7 (Supplementary Figure S11C), whereas occasional colocalization of TGN46 with PS-ASOs at LE could be observed after PS-ASO cellular uptake (Supplementary Figure S11D), despite the fact that TGN46 does not bind PS-ASOs (Supplementary Figure S9A). These observations suggest that TGN46 may be involved in PS-ASO endosomal trafficking and/or release. Both TGN46 and Golgi-58K could colocalize at Golgi region (Supplementary Figure S12A), however, much fewer TGN46/PS-ASO colocalization was found as compared with PS-ASO-Golgi-58K colocalization (Supplementary Figure S12B). These results, together with our previous findings that STX5-COPII pathway and GCC2-M6PR pathway facilitate PS-ASO endosomal release (14,20), suggesting that the Golgi may play an important role in mediating PS-ASO action, and that different Golgi proteins may have different influence. Since Golgi-58K showed robust relocalization to LEs upon cellular uptake of PS-ASOs, we further characterized the potential underlying mechanisms by which this protein affects PS-ASO activity.

The LE localization of Golgi-58K upon PS-ASO incubation is time and PS-ASO concentration dependent

Previously, we found that recruitment of different proteins to LEs occurs at different times after PS-ASO incubation with cells. For example, it takes approximately 2–4 h for ANXA2 relocalization to LEs (13), and 4–6 h for STX5 and GCC2 recruitment to LEs after PS-ASO incubation (14,20). These relocalization times are slightly earlier than those times required for PS-ASO-mediated target reduction, as it usually takes more than 6–8 h for decent degradation of target RNAs, as exemplified with two PS-ASOs targeting nuclear Malat1 and U16 RNAs, and one ASO targeting cytoplasmic *Drosha* mRNA (Figure 4A). To determine the kinetics of Golgi-58K relocalization to LEs, Cy3-PS-ASO was incubated with HeLa cells at 2 μM for different times, and cells were stained for Golgi-58K (Figure 4B, C and data not shown). Colocalization of Gogi-58K with PS-ASOs was rarely detectable 4 h after PS-ASO incubation, but substantially increased over time, from less than 5 per cell at 4 h to over 20 per cell at 10 h after PS-ASO incubation. Time dependent colocalization was also determined by analyzing Pearson's correlation coefficient (Supplementary Figure S13A). These results indicate that similar to other LE relocated proteins, Golgi-58K recruitment to LEs is also time-dependent, with detectable co-localization at 4–8 h. This relocalization kinetics is correlated with the times exhibiting low but detectable PS-ASO activity upon free uptake. Since the released PS-ASOs may take as short as 30 min to trigger target RNA degradation, as we determined previously by transfection (7), the early relocalization of Golgi-58K to LEs may facilitate ASO release from endosomes, contributing to the observed antisense activity.

Since PS-ASOs can achieve antisense activity at lower concentrations than 2 μM as used in imaging assays, next, we evaluated the Golgi-58K colocalization with PS-ASOs at low concentrations. HeLa cells were incubated with Cy3-PS-ASOs for 16 h at concentrations ranging from 0.1 to 0.8 μM. Immunofluorescence staining results showed that even at 0.1 μM, colocalization between PS-ASO and Golgi-58K was readily detectable (Figure 4D). Quantification showed that the colocalization events and Pearson's correlation coefficient increased with higher PS-ASO concentrations (Figure 4E and Supplementary Figure S13B), suggesting a dose dependent relocalization of Golgi-58K protein. Together, these results indicate that even at low concentrations of PS-ASOs, Golgi-58K protein can still relocate to LEs.

Reduction of Golgi-58K caused slower endosomal release of PS-ASOs

Next, we evaluated the effects of reduction of Golgi-58K on PS-ASO internalization and endocytic trafficking. Similar levels of internalized PS-ASOs were detected in control and Golgi-58K reduced cells, as determined by quantifying internalized Cy3-PS-ASO signal at 4 h after PS-ASO incubation (Figure 5A), indicating that Golgi-58K reduction did not substantially affect PS-ASO uptake. In addition, PS-ASO localization to LEs was also not affected by reduction of this protein, as shown by confocal imaging of cells at 3 h after PS-ASO incubation (Figure 5B), suggesting that Golgi-58K may not be required for PS-ASO transport to LEs. Consistently, reduction of Golgi-58K did not affect PS-ASO co-localization with ANXA2 (Supplementary Figure S14A, B), a protein that is recruited to LEs upon PS-ASO uptake and is required for EE to LE transport and LE release of PS-ASOs (13,19).

To determine whether Golgi-58K affects LE release of PS-ASOs, HeLa cells treated with control or Golgi-58K-specific siRNAs were incubated with the *Drosha*-targeting PS-ASO for 2 h to ensure sufficient uptake of PS-ASOs for antisense activity. Medium was then changed to remove extracellular PS-ASOs and to eliminate further uptake (Figure 5C, upper panel), as we described previously (13,14). Cells were then collected at different times after PS-ASO removal and the levels of targeted *Drosha* mRNA was determined by qRT-PCR (Figure 5C, lower panel). The results showed that reduction of Golgi-58K decreased PS-ASO activity under these conditions. As PS-ASO uptake is not affected by reduction of Golgi-58K and internalized PS-ASOs can pass through EE and enter LE within 1–2 h (13), the decreased PS-ASO activity after PS-ASO removal should mainly reflect slower PS-ASO release from LEs.

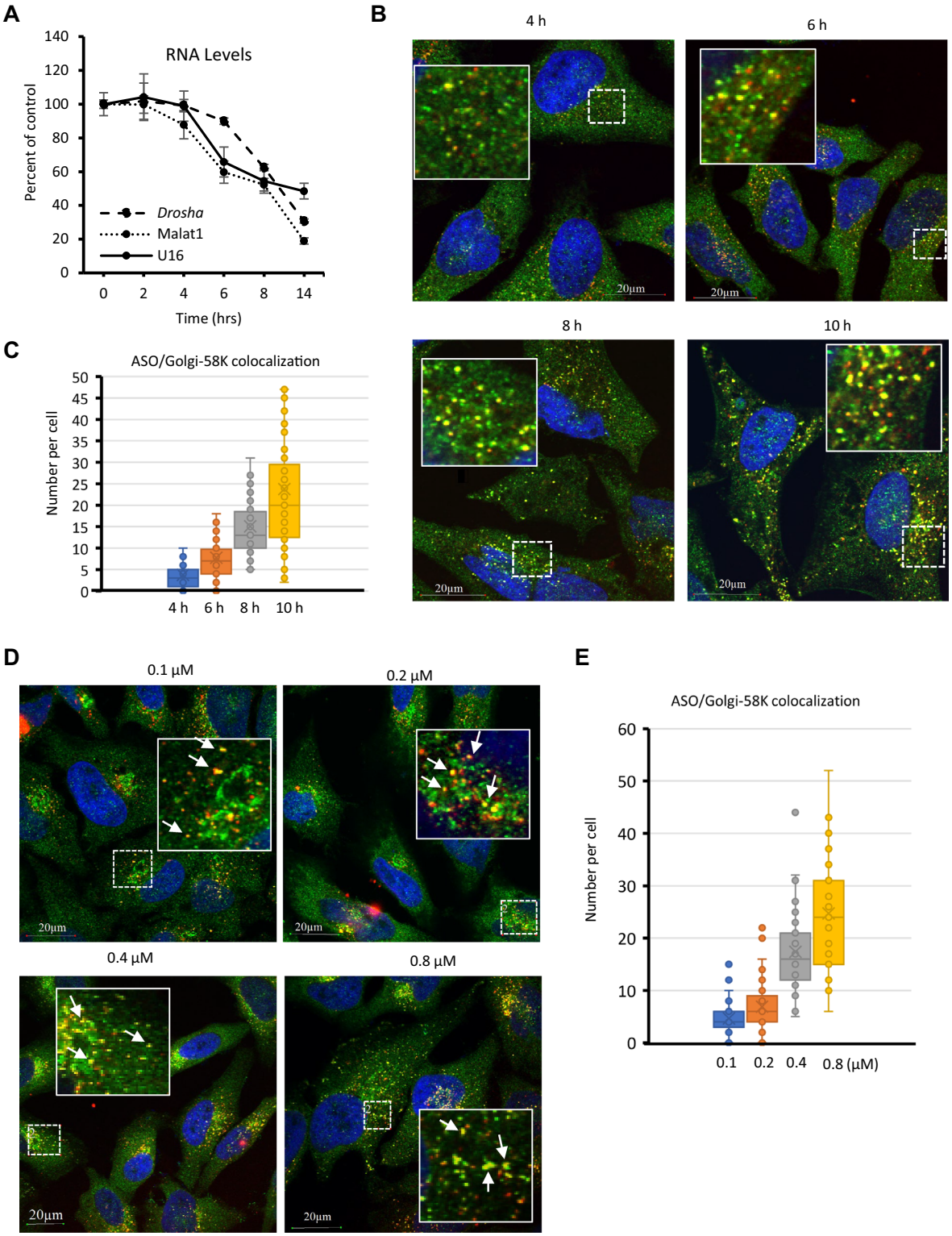

Figure 4. The kinetics of Golgi-58K relocalization to LEs correlates with the kinetics of PS-ASO activity. (**A**) qRT-PCR quantification of *Malat1* and *U16* RNAs in HeLa cells incubated for different times with 1 μM PS-ASO 395254 or 5 μM PS-ASO 462026 targeting these RNAs, respectively. Error bars represent standard deviations from three independent experiments. The colocalization times of ANXA12 and COPII proteins with PS-ASOs at LEs as determined previously are indicated below the X-axis. (**B**) Immunofluorescence staining of Golgi-58K in HeLa cells incubated with 2 μM Cy3-labeled PS-ASO 446654 for different times. Scale bars, 20 μm. (**C**) Quantification of PS-ASO-Golgi-58K colocalization events in cells incubated with PS-ASOs for different times, as exemplified in panel B. Colocalizations was counted in ∼25 cells and average values and standard deviations are plotted. (**D**) Immunofluorescence staining of Golgi-58K in HeLa cells incubated with different concentrations of Cy3-labeled PS-ASO 446654 for 16 h. Scale bars, 20 μm. (**E**) Quantification of PS-ASO-Golgi-58K colocalization events in cells as exemplified in panel D. Colocalization was counted in ∼25 cells and average values and standard deviations are plotted.

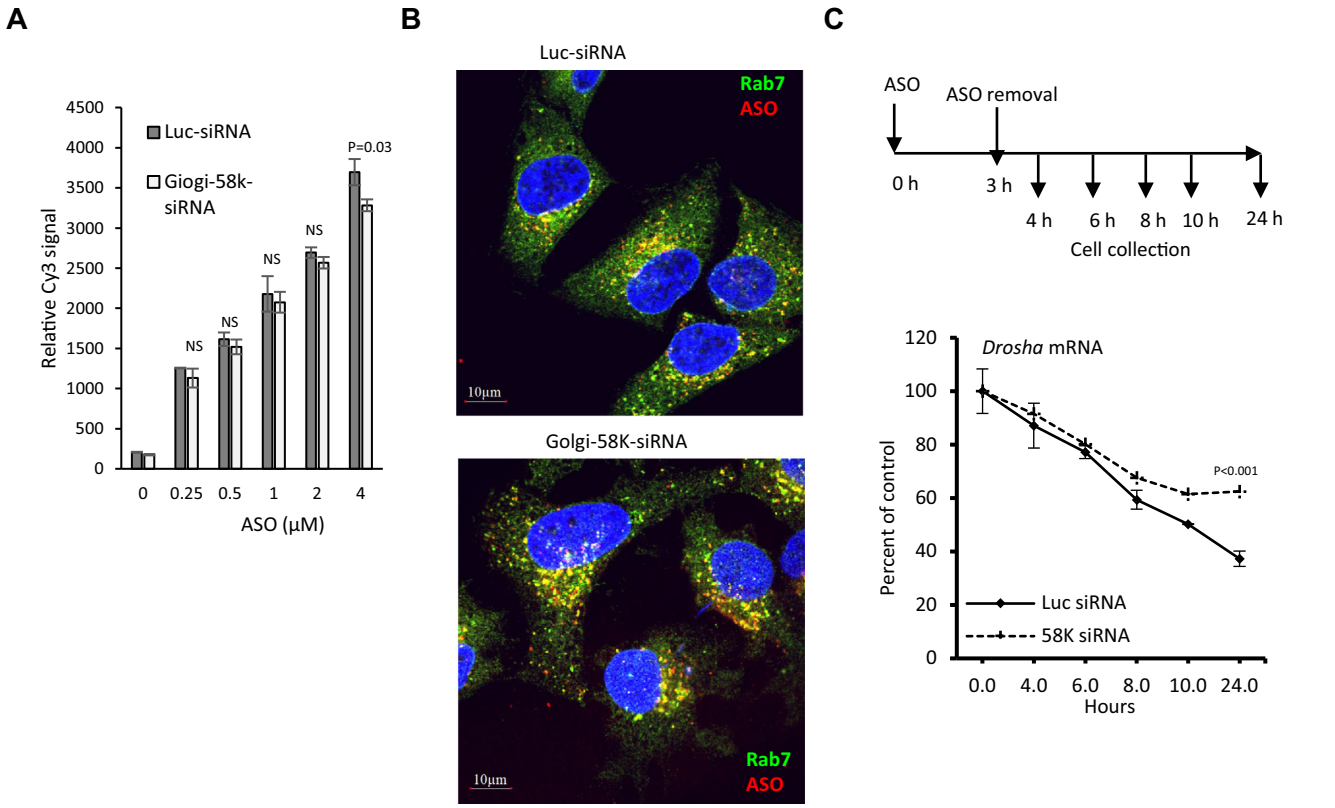

Figure 5. Reduction of Golgi-58K caused slower endosomal release of PS-ASOs. (**A**) Quantification of PS-ASO uptake in control or Golgi-58K reduced HeLa cells. As described in Materials and Methods section. Error bars represent standard deviation of three experiments. (**B**) Immunofluorescence staining of Rab7 in HeLa incubated with 2 μM Cy3-labeled PS-ASO 446654 for 3 h. Scale bars, 10 μm. (**C**) qRT-PCR quantification of the levels of *Drosha* mRNA in HeLa cells. Cells pretreated with control luciferase siRNA, or siRNAs targeting *Golgi-58K* were incubated with 20 μM PS-ASO25690 for 3 h. Medium containing PS-ASO was then replaced with fresh medium. and RNA levels were quantified at indicated time points, as shown in the upper panel. Error bars are standard deviations from three independent experiments. *P* values were calculated based on *F*-test.

To further confirm that Golgi-58K reduction hinders PS-ASO endosomal release, a Cy3-PS-ASO was incubated for 16 h with GFP-Rab7 expressing SVGA cells pre-treated with control or Golgi-58K siRNAs for 48 h. Live cell movies were then taken using confocal microscope, and the Cy3 signal in perinuclear area that enriches LEs were measured over time, as exemplified in Supplementary Figure S15A. Cy3-PS-ASO release from LEs should lead to reduction in Cy3 signal in the LE-enriched areas over time. Quantification results showed that Golgi-58K reduction led to a slower signal decline as compared with that in control cells (Supplementary Figure S15B). Similarly, Cy3-PS-ASO signal was also measured from the nucleus that represents PS-ASOs released from endosomes, as exemplified in Supplementary Figure S15C. Golgi-58K reduction caused slower increase in the nuclear PS-ASO signal (Supplementary Figure S15D). Altogether, these results indicate that reduction of Golgi-58K impaired PS-ASO release from endocytic organelles.

Golgi-58K colocalizes with PS-ASOs inside LEs and on LE membranes

To evaluate the potential mechanisms of Golgi-58K-mediated endosomal release of PS-ASOs, immunofluorescence staining was performed in GFP-Rab7 expressing SVGA cells incubated with Cy3- PS-ASOs. In some LEs, PS-ASOs were not evenly distributed but appeared as distinct foci most likely as intralumenal vesicles (ILVs), as we determined previously by co-staining of the intralumenal PS-ASOs with LBPA, a lipid enriched in the membranes of LEs and ILVs (17,20). Interestingly, Golgi-58K could also be detected by both 2D and 3D imaging as distinct foci inside LEs and colocalized with PS-ASOs (Figure 6A, Supplementary Movie S1), suggesting that Golgi-58K is present at ILVs. Signal intensity profile also showed co-peaks of PS-ASO and Golgi-58K inside LEs (Figure 6A, right panel). Since a GFP-tagged Golgi-58K failed to correctly localize to Golgi (data not shown), the co-movement of distinct PS-ASO foci inside LEs was recorded in live cells expressing GFP-Rab7 (Supplementary Movie S2). In addition, Golgi-58K could also be detected as distinct, vesicle-like structures on the limiting membranes of certain LEs containing PS-ASOs, as shown also by the signal intensity profiles and Z-section imaging (Figure 6B, Supplementary Movie S3), similar to the case of M6PR vesicles (20). These observations suggest possibilities that Golgi-58K may facilitate PS-ASO release from LEs, likely through different pathways, such as release through back-fusion process mediated by ILVs and vesicle-mediated escape of PS-ASOs from LEs.

It has been shown that some proteins, including GCC2 and COPII complex proteins, can relocate to LEs upon

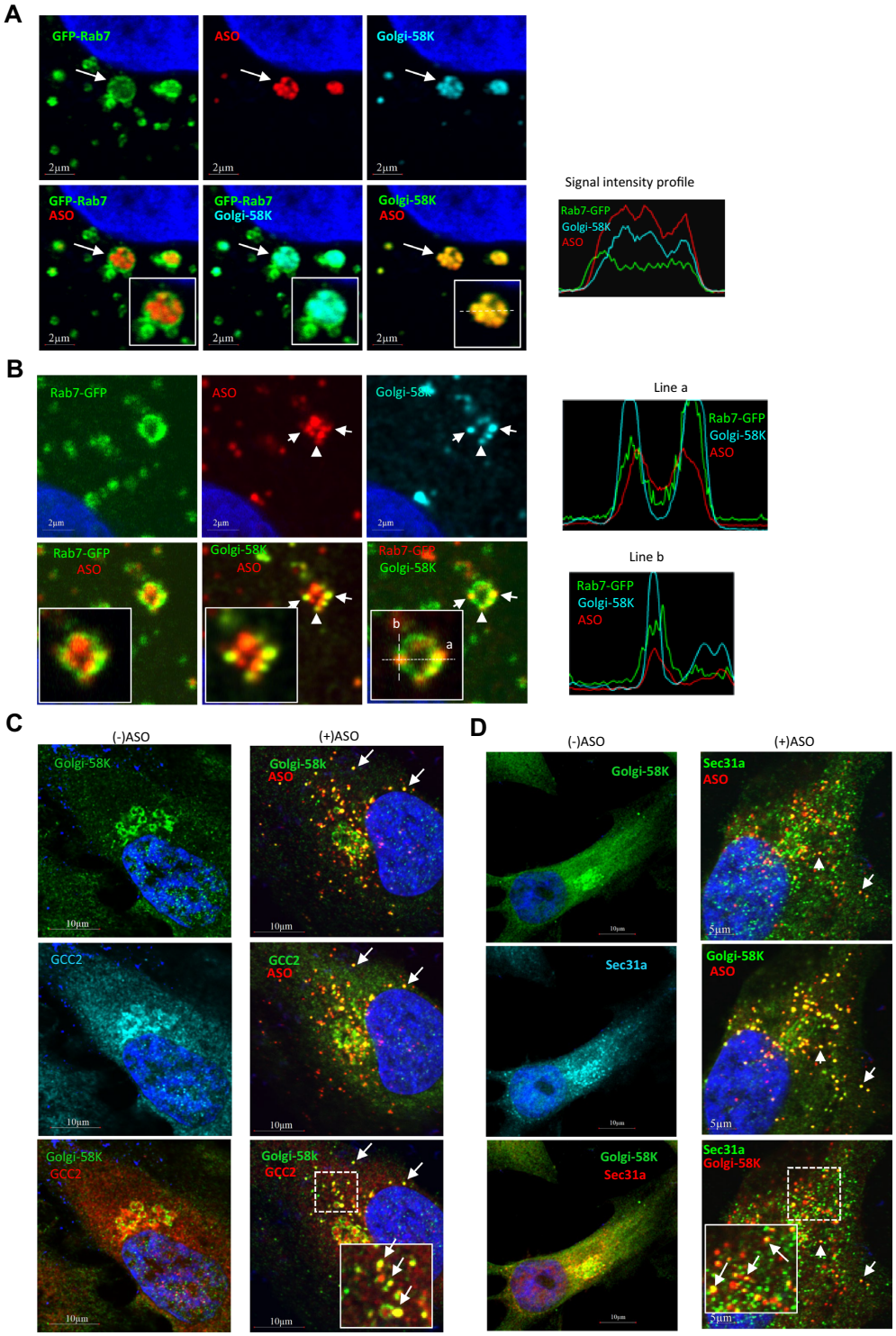

Figure 6. Golgi-58K can localize at different loci of LEs and can co-localize with GCC2 and COPII proteins upon PS-ASO free uptake. (**A**) Immunofluorescence staining of Golgi-58K in GFP-Rab7-expressing SVGA cells incubated with 2 μM Cy3-labeled PS-ASO 446654 for 16 h. Golgi-58K colocalization with PS-ASOs as distinct foci within LEs are marked with arrows. Scale bars, 2 μm. Enlarged images of the LE are shown in islets. The signal intensity profile from the line across the LE is shown in right panel. (**B**) Immunofluorescence staining of Golgi-58K as in panel A. An example of Golgi-58K localization as distinct foci on the membrane of LEs is marked with arrows. Scale bars, 2 μm. Enlarged images of the LE are shown in islets. Lines a and b in the box indicate the sections for signal intensity profiles as shown in right panels. (**C**) Immunofluorescence staining of Golgi-58K and GCC2 in HeLa cells incubated [(+) ASO] or not incubated [(-)ASO] with 2 μM Cy3-labeled PS-ASO 446654 for 16 h. Arrows exemplify colocalization between the two proteins and with PS-ASOs. A boxed area was magnified and shown in islet. Scale bars, 10 μm. (**D**) Immunofluorescence staining of Golgi-58K and Sec31a in HeLa cells incubated [(+) ASO] or not incubated [(-)ASO] with 2 μM Cy3-labeled PS-ASO 446654 for 16 h. Arrows exemplify colocalization between the two proteins and with PS-ASOs. A boxed area was magnified and shown in islet. Scale bars, 10 μM and 5 μm for left and right panels, respectively.

PS-ASO cellular uptake (14,20). To determine if Golgi-58K colocalizes with these proteins at LEs, immunofluorescence staining was performed in cells incubated with Cy3-PS-ASOs. In the absence of PS-ASOs, Golgi-58K and GCC2 stained the Golgi region, as expected, and no scattered foci in the cytoplasm were detected (Figure 6C, left panel). Upon PS-ASO cellular uptake, Golgi-58K colocalized with PS-ASO and GCC2 in cytoplasmic dot-like foci (Figure 6C, right panel), most likely LEs, since both Golgi-58K and GCC2 relocate to LEs upon PS-ASO uptake (20). Colocalization of Golgi-58K with GCC2 in PS-ASO containing foci was also determined through Pearson's correlation coefficient analysis (Supplementary Figure S16A). Golgi-58K does not obviously colocalize with Sec31a, a COPII protein, in cytoplasmic foci in cells without PS-ASO incubation (Figure 6D, left panel). However, colocalization of Golgi-58K and Sec31a in cytoplasmic foci could be readily detected after PS-ASO cellular uptake (Figure 6D, right panel). Pearson's correlation coefficient analysis also showed modest colocalization of Golgi-58K with Sec31a in PS-ASO foci (Supplementary Figure S16B). Together, these results indicate that upon PS-ASO uptake, Golgi-58K can be recruited to LEs, either in ILVs, or on the membrane of LEs, and can colocalize with other proteins that re-localize to LEs, such as GCC2 and COPII proteins.

Reduction of Golgi-58K decreased GCC2 relocalization to LEs upon PS-ASO cellular uptake

Previous we have shown that GCC2-M6PR pathway and STX5-COPII pathways act independently to facilitate endosomal release of PS-ASOs (20). To determine whether Golgi-58K is involved in these two transport pathways, PS-ASO colocalization with GCC2 or with Sec31a was analyzed through immunofluorescence staining in control or Golgi-58K siRNA treated cells. Without PS-ASO incubation, reduction of Golgi-58K did not affect the Golgi localization pattern of GCC2 (Figure 7A). However, upon PS-ASO cellular uptake, significantly less GCC2-PS-ASO colocalization was detected in Golgi-58K reduced cells, when compared to control cells (Figure 7B–D), although PS-ASO-ANXA2 colocalization was not affected under the same conditions (Figure 7B, C, Supplementary Figure S14). Similar results were also observed using Pearson's correlation coefficient assay (Supplementary Figure S16C). In contrast, reduction of GCC2 did not significantly affect PS-ASO-Golgi-58K colocalization (Supplementary Figure S17), suggesting that Golgi-58K acts at a step preceding GCC2. Though GCC1 and TGN46 are involved in TGN-Endosomal transport, reduction of GCC1 or TGN46 did not abolish PS-ASO-GCC2 colocalization (Supplementary Figure S18).

On the other hand, the cellular localization of Sec31a and PS-ASO-Sec31a colocalization were not significantly affected by Golgi-58K reduction (Supplementary Figure S19). Reduction of Sec31a also did not affect PS-ASO-Golgi-58K colocalization (Supplementary Figure S20). These results suggest that Golgi-58K is not involved in COPII-mediated PS-ASO release process. This is consistent with our previous findings that COPII pathway and GCC2-M6PR pathway are independent pathways affecting PS-ASO release from LEs.

Golgi-58K relocalization to LEs requires Hsc70 and may affect retrograde transport of M6PR

Recently we found that a heat shock protein, Hsc70, is involved in M6PR shuttling between LE and TGN by facilitating M6PR vesicle budding from LEs (25). Reduction of Hsc70 decreased PS-ASO-GCC2 colocalization at LEs. Since reduction of Golgi-58K also impaired GCC2-PS-ASO colocalization, we next evaluated whether reduction of Hsc70 affects PS-ASO-Golgi-58K colocalization, that may subsequently affect GCC2 relocalization. Hsc70 protein was reduced in HeLa cells by siRNA treatment (Figure 8A), and the PS-ASO-Golgi-58K colocalization pattern was determined by immunofluorescence staining. Reduction of Hsc70 did not affect Golgi integrity (25), or Golgi-58K localization in the absence of PS-ASOs (Supplementary Figure S21). However, after PS-ASO cellular uptake, Golgi-58K colocalization with PS-ASOs was dramatically decreased in Hsc70 reduced cells as compared with that in control cells (Figure 8B, C), indicating that Hsc70 is involved in Golgi-58K relocalization to LEs upon PS-ASO uptake.

Since Golgi-58K affects PS-ASO-GCC2 colocalization and not vice versa, it is possible that Golgi-58K may affect GCC2 function, for example, in M6PR shuttling. To evaluate this possibility, HeLa cells treated with either control or Golgi-58K siRNA were incubated for 75 min with an antibody specific to the cation independent M6PR (M6PR-CI) that recognizes the extracellular domain of the protein. M6PR-CI antibody can be internalized via M6PR-CI, and transport through LEs to TGN (40). Thus, it is able to monitor the intracellular transport of M6PR, as we described previously (25). Immunofluorescence staining of the M6PR-CI antibody, and quantification of the localization of the antibody in LEs showed that reduction of Golgi-58K modestly increased LE retention of M6PR-CI antibody, as compared with that in control cells (Figure 8D,E). The modestly increased LE retention of M6PR-CI antibody was also detected by analyzing Pearson's correlation coefficient (Supplementary Figure S22). This experiment was repeated three times (Supplementary Figure S23 and data not shown), and similar observation was made, suggesting that the defect, though modest, is highly reproducible. These results suggest that Golgi-58K reduction caused slower retrograde transport of M6PR from LE to TGN, implying a biological role of Golgi-58K in this transport pathway.

Golgi-58K relocalization to LEs may be mediated by PS-ASO-protein interactions

Previously we showed that the relocalization of STX5 and GCC2 to LEs may be mediated by PS-ASO-protein interactions, since the degree of protein relocalization to LEs upon PS-ASO incubation positively correlates with the binding affinity of the PS-ASOs to proteins (14,20). The PS-ASO-induced Golgi-58K relocalization to LEs may thus also be mediated by PS-ASO-protein interactions, either directly,

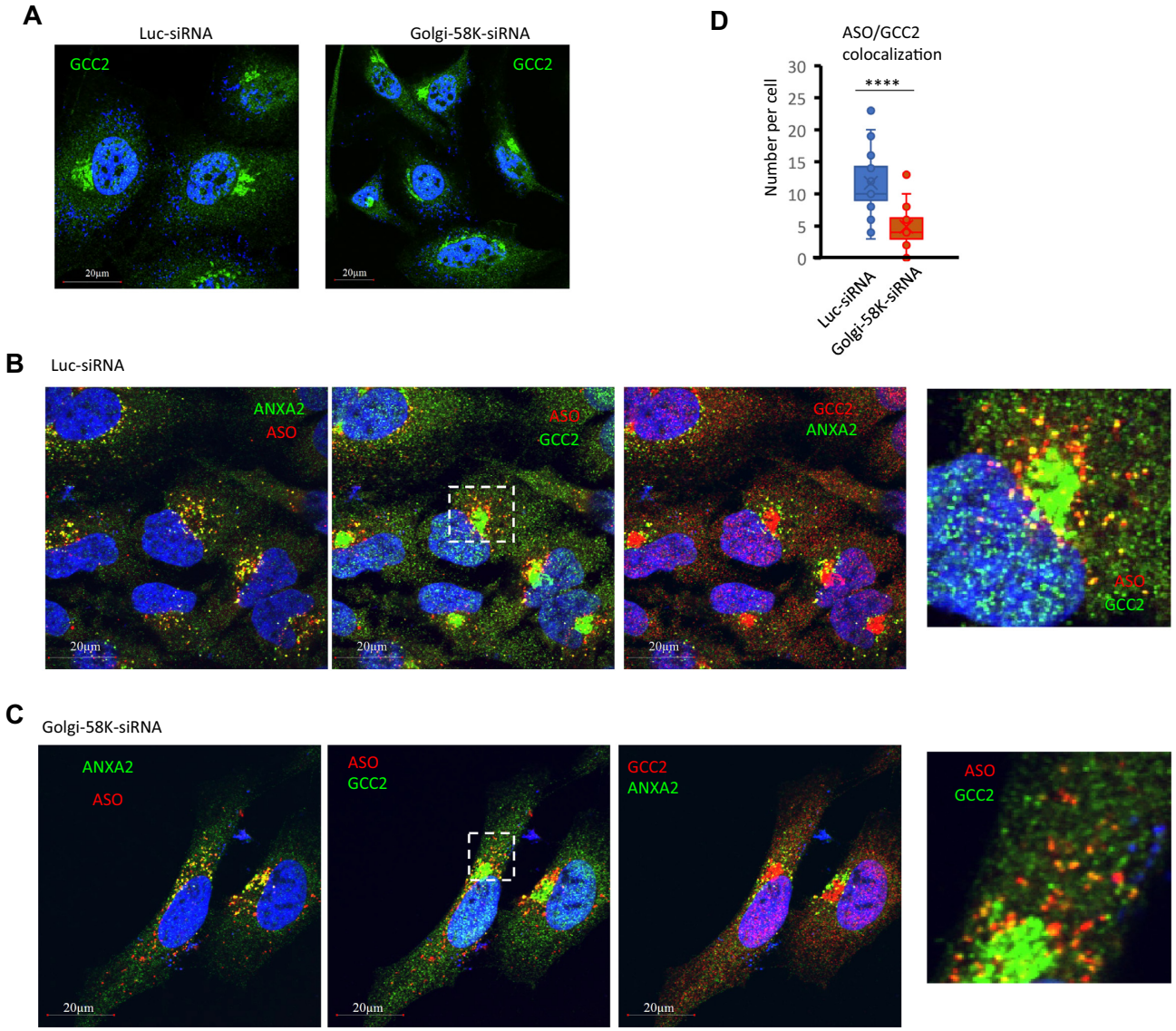

Figure 7. Reduction of Golgi-58K impaired PS-ASO-GCC2 colocalization. (**A**) Immunofluorescence staining of GCC2 in HeLa cells treated with control or Golgi-58K specific siRNAs. (**B-C**) Immunofluorescence staining of ANXA2 and GCC2 in luciferase siRNA treated (Panel B) or Golgi-58K siRNA treated (Panel C) HeLa cells that were incubated with 2 μM Cy3-labeled PS-ASO 446654 for 16 h. An area of PS-ASO-GCC2 merged panel was magnified and shown in right panels. (**D**) Quantification of PS-ASO-GCC2 colocalization in control or Golgi-58K reduced cells, as shown in panels B and C. Error bars are standard deviations from ∼20 cells. *P* value was calculated based on unpaired *t*-test. ****$P<0.0001$.

or mediated by other PS-ASO binding proteins. The ASOs used above are all modified with PS backbones, which dramatically increases protein binding as compared with phosphodiester (PO) backbone ASOs (6,27,41). To determine if Golgi-58K protein is able to bind PS-ASOs, affinity selection was performed using biotinylated PS-ASOs or PO-ASOs, incubated with purified recombinant Golgi-58K protein, since the endogenous protein level is low in these cells. Western results showed that Golgi-58K protein was significantly co-isolated with the PS-ASO, and not the PO-ASO (Figure 8F), suggesting that this protein can directly bind PS-ASOs.

To evaluate if PS-ASO-protein interaction is involved in Golgi-58K relocalization to LEs, 2 μM GalNAc-conjugated PS-ASO or PO-ASO was incubated with HepG2 cells that express ASGR protein, through which GalNAc-conjugated ASOs can enter cells (9,42). Indeed, while both GalNAc-PS-ASO and GalNAc-PO-ASO entered cells to comparable levels, only GalNAc-PS-ASO colocalized with Golgi-58K protein (Figure 8G, H), suggesting that Golgi-58K relocalization to LEs is most likely mediated by PS-ASO–protein interactions. In addition, colocalization of Golgi-58K with GalNAc-PS-ASO was also observed at low concentration (0.1 μM), and the colocalization event increased with higher GalNAc-PS-ASO concentrations (Supplementary Figure S24), consistent with what was observed with unconjugated PS-ASOs in HeLa cells.

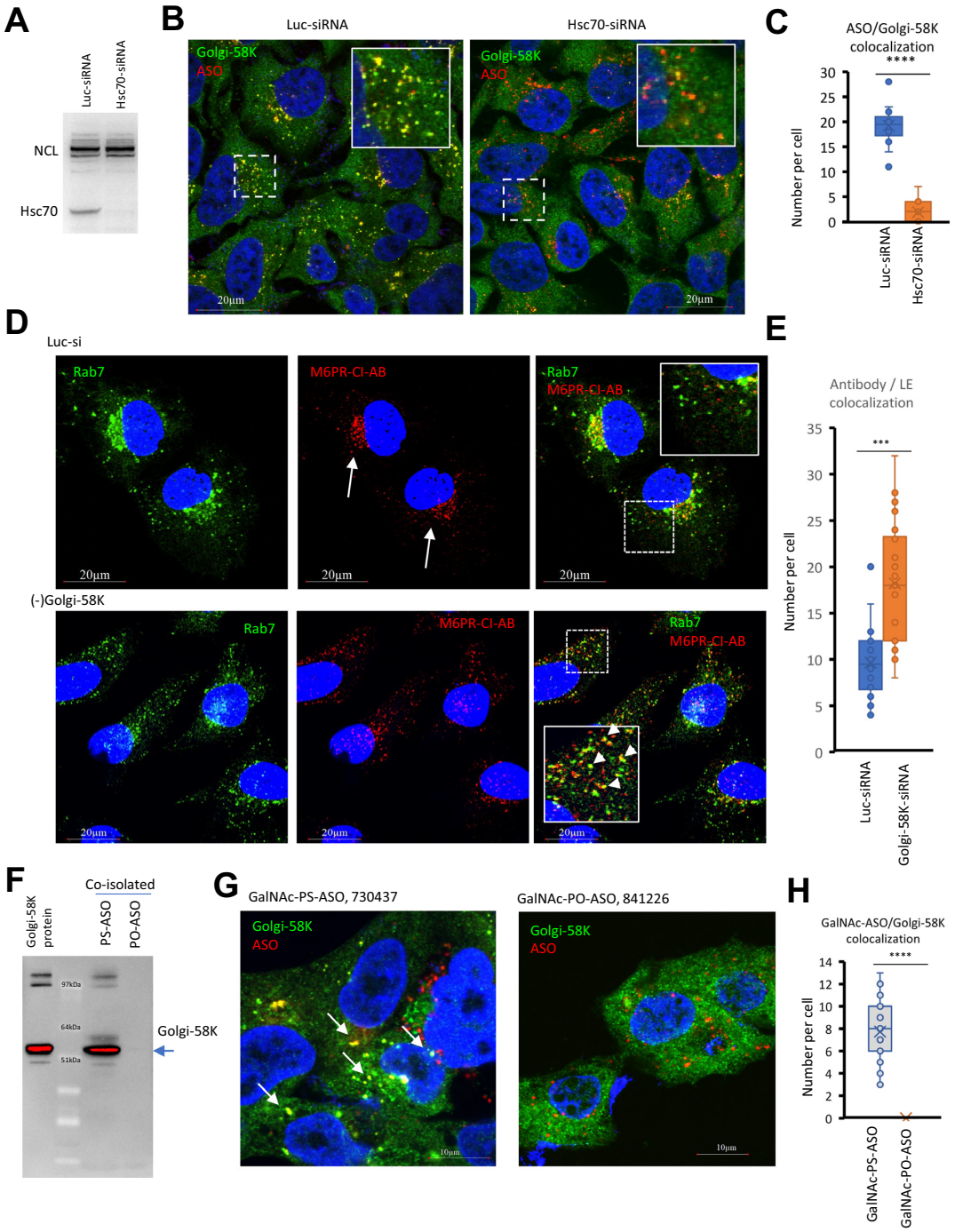

Figure 8. Golgi-58K relocalization to LEs requires Hsc70 and may be mediated by PS-ASO-protein interactions. (**A**) qRT-PCR quantification of *Hsc70* mRNA in HeLa cells transfected with different siRNAs for 48 h. (**B**) Immunofluorescence staining of Golgi-58K in control or Hsc70 reduced HeLa cells incubated with 2 μM Cy3-labeled PS-ASO 446654 for 16 h. (**C**) Quantification of PS-ASO-Golgi-58K colocalization in control or Hsc70 reduced cells, as shown in panel B. Error bars are standard deviations from ∼20 cells. *P* value was calculated based on unpaired *t*-test. ****$P < 0.0001$. (**D**) Immunofluorescence staining of M6PR-CI antibody and Rab7 in control and Golgi-58K reduced HeLa cells. The M6PR-CI antibody was incubated with cells at 4°C for 20 min, followed by incubation at 37°C for 75 min, as described in Materials and Methods. The perinuclear localization of the antibody is marked with arrows in control cells. Scale bars, 20 μm. The boxed areas are shown as islets. The antibody-containing scattered LEs are marked with arrowheads. (**E**) Quantification of LE-localized M6PR antibody in control or Golgi-58K reduced cells, as in panel D. M6PR-CI antibody stained LEs were counted manually from ∼25 cells in each case, and the average values and standard deviations are plotted. *P* value was calculated based on unpaired *t*-test. ***$P < 0.001$. (**F**) Western analysis for Golgi-58K protein. Affinity selection using biotinylated-ASOs were performed as described in Materials and Methods section, and selected proteins were separated on SDS-PAGE and detected by western blotting. (**G**) Immunofluorescence staining of Golgi-58K in HepG2 cells incubated with 2 μM GalNAc-conjugated ASO containing either PS backbone (left panel) or PO backbone (right panel) for 16 h. Colocalization between GalNAc-PS-ASO and Golgi-58K was exemplified with arrows. (**H**) Colocalization between Golgi-58K and GalNAc-ASOs as exemplified in panel G was counted from ∼25 cells, and average values and standard deviations are plotted. *P* value was calculated based on unpaired *t*-test. ****$P < 0.0001$.

DISCUSSION

In this study, we further characterized the potential roles of Golgi in PS-ASO trafficking and activity. We found that some Golgi proteins, including Golgi-58K, TGN46, GCC1 and Man2A1, affect the antisense activities of PS-ASOs. These results, together with our previous observations, suggest that Golgi components can positively affect PS-ASO activity, most likely by facilitating PS-ASO intracellular distribution and endosomal release. In addition, we also found that Golgi-58K facilitates endosomal release of PS-ASOs, affects GCC2 relocalization to LEs upon PS-ASO incubation, and modestly affects M6PR transport, suggesting a novel function of Golgi-58K in TGN-endosome transport. Consistent with our previous observations that reduction of a particular protein typically causes modest defects on PS-ASO activity (6,11), depletion of these Golgi proteins, including Golgi-58K, also led to modest reduction in PS-ASO activity. These observations further indicate that multiple pathways or protein factors can act in parallel to contribute to PS-ASO release, thus blocking one pathway only causes partial defects. These results also highlight the complexity of PS-ASO release mechanism, which is important for the development of approaches to enhance PS-ASO release.

Golgi apparatus are involved in protein modification and vesicular transport of cellular components, either to other cellular organelles, secreted to extracellular environments through anterograde transport, or through retrograde transport by which materials can be transported from plasma membrane and endosomes to Golgi and to ER. These intrinsic transport pathways, especially retrograde transport from endosomes to TGN, have been shown to be utilized by extracellular materials including virus and toxins to enter cells (43,44). Similarly, PS-ASOs can also utilize Golgi-mediated transport pathways to escape the endosomal organelles. GCC2-mediated M6PR shuttling between LEs and TGN has been shown to facilitate endosomal release of PS-ASOs (20). In addition, STX5, which normally localizes at Golgi to tether incoming COPII vesicles derived from ER (45), can facilitate PS-ASO release from LEs through COPII vesicles (14). Here we showed that additional Golgi proteins, including TGN46, GCC1, Man2A1, and Golgi-58K, also participate in productive PS-ASO trafficking and release, further highlighting the importance of Golgi in PS-ASO activity.

However, not all tested Golgi proteins affect PS-ASO activity. For example, no substantial effect on PS-ASO activity was observed upon reduction of STX6, STX16 (14), GM130 (20), TMED9 and TMED10. This is not unexpected due to the multiple different roles of Golgi in protein maturation, sorting and transport, and since different proteins may have distinct functions in mediating transport in and out of Golgi. Although TMED9 and TMED10 are involved in shuttling of COP I/II vesicles between ER and Golgi, reduction of TMED9, TMED10, as well as COP I proteins did not substantially affect PS-ASO activity (14). These observations suggest that ER-to-Golgi transport seems not directly involved in PS-ASO endosomal release, or subcellular distribution. Consistently, although COPII vesicles can relocate to LEs upon PS-ASO cellular uptake and facilitate ASO release, we have demonstrated that de novo formation of COPII vesicles on ER membrane is not required and that COPII vesicles that re-localized to LEs after PS-ASO uptake are most likely pre-existing vesicles (14).

On the other hand, TGN-Endosome shuttling appears to play important roles in PS-ASO trafficking and release. Recently, we showed that GCC2-mediated M6PR shuttling between TGN and LEs significantly facilitates PS-ASO endosomal release (20). Here, we found that reduction of GCC1 and TGN46 also modestly impaired PS-ASO activity. It has been demonstrated that GCC1 mediates TGN46 transport mostly from EEs to TGN (35), but not M6PR shuttling from LE to TGN, which is mediated by GCC2 protein (35,36). Indeed, we found that TGN46 can localize to EEs, suggesting a possibility that TGN46 may contribute to PS-ASO release from EEs. The very modest effects of TGN46/GCC1 reduction on PS-ASO activity was not unexpected, as it has been shown that LEs or MVBs are the major sites for productive PS-ASO release (11). Upon PS-ASO cellular uptake, TGN46 was also detected occasionally colocalizing with PS-ASOs at LEs, suggesting that TGN46 and GCC1 proteins may be weakly involved in PS-ASO release from LEs. Since GCC2-PS-ASO colocalization was not affected by reduction of GCC1 or TGN46, it is likely that GCC2-M6PR pathway and GCC1-TGN46 pathway may act independently on PS-ASO trafficking from endosomes and TGN. Dissecting the underlying mechanisms by which TGN46-GCC1 proteins affect PS-ASO activity awaits further investigation.

Although PS-ASO uptake caused significant LE relocalization of Golgi-58K, as determined by confocal staining, the actual fraction of relocalized Golgi-58K protein relative to total cellular Golgi-58K is unclear, since confocal imaging is not very quantitative and the signal intensities of LE enriched Golgi-58K and more diffused Golgi-localized Golgi-58K are very different, making it difficult to quantify the level of relocalized Golgi-58K proteins. However, based on our previous observations, intense fluorescence signal does not necessarily indicate high level of the relocalized proteins. For example, TCP1β, a cytoplasmic protein, exhibited very strong nuclear PS body localization upon PS-ASO transfection by immunofluorescence staining, however, subcellular fractionation results indicated that only a very tiny fraction of the protein was relocalized to the nucleus (27). Similarly, ANXA2, which was found by immunofluorescence staining to significantly relocate to LEs upon PS-ASO free uptake, only showed very modest relocalization to LEs in fractionation experiments (13). These results suggest that the actual level of LE relocalized Golgi-58K protein may not be as high as seen from the confocal imaging. This possibility is also supported by our observations that incubation of PS-ASOs even at high concentration (10 μM) did not affect normal cell growth and the levels of secreted glycoproteins (14), indicating that incubation of PS-ASOs did not disrupt normal Golgi (and cellular) functions.

Interestingly, reduction of Golgi-58K significantly impaired PS-ASO activity upon free uptake, due to slower release from LEs. It is possible that Golgi-58K may enhance PS-ASO release from LEs through a back-fusion process

mediated by ILVs, as this protein can colocalize with PS-ASOs in distinct foci inside LEs, similar to ANXA2 and GCC2 proteins (13,20). Additionally, it is also possible that Golgi-58K mediates PS-ASO release through vesicles, since Golgi-58K can also be observed as vesicle-like localization pattern on LE membranes. Golgi-58K has been reported to be involved in protein modification, however, the role of this protein in Golgi-related transport has also been implicated (46). For example, Golgi-58K can bind microtubules and may mediate interactions of TGN-derived vesicles with microtubules (46,47). Here, we found that Golgi-58K can relocate to LEs upon PS-ASO uptake most likely mediated by ASO-protein interactions, similar to GCC2 and STX5 proteins (14,20). Reduction of Golgi-58K dramatically reduced LE recruitment of GCC2 upon PS-ASO uptake, but not vice versa, suggesting that Golgi-58K acts upstream of GCC2 in mediating PS-ASO transport and endosomal release. Similarly, reduction of GCC1 or TGN46 did not affect Golgi-58K-PS-ASO colocalization at LEs, suggesting these proteins are not involved in Golgi-58K mediated transport process.

On the other hand, Hsc70 has been shown to be required for GCC2 relocalization to LEs upon PS-ASO uptake (25). Hsc70 can bind PS-ASOs and can compete with RNase H1 for binding to PS-ASO/RNA duplex (19,48). This protein also relocates to the nucleolus after prolonged treatment with toxic PS-ASOs that can trigger phase separation of the nucleolar structures (49). Here we found that reduction of Hsc70 abolished Golgi-58K relocalization to LEs. These observations suggest a cluster events of protein action. It is likely that upon PS-ASO uptake, Hsc70 mediates Golgi-58K relocalization to LEs, and subsequently Golgi-58K mediates GCC2 relocalization to LEs to facilitate PS-ASO release either directly, or mediated by M6PR vesicles. However, Hsc70 is also required for M6PR vesicle budding from LE membranes, as we recently reported (25), suggesting versatile roles of this chaperon protein.

Together, these results suggest important roles of Golgi in mediating endosomal release of PS-ASOs, a limiting step in ensuring PS-ASO activity. Though different proteins, or pathways of the Golgi network may be involved, the M6PR shuttling pathway between TGN and LEs that is mediated by Hsc70, Golgi-58K, and GCC2 appears to have significant influence on productive PS-ASO release, which is most likely mediated by PS-ASO-protein interactions (6,11). Currently it is unclear how Golgi-58K and other proteins such as STX5 and GCC2 are recruited to LEs upon PS-ASO cellular uptake, since PS-ASOs are present inside LE limiting membranes and these cellular proteins exist mostly in the cytosolic side. It is possible that PS-ASOs in LEs interact with the luminal domain(s) of some LE membrane proteins, leading to conformational change of the cytosolic domain(s) of the proteins, that in turn facilitates the recruitment of Golgi-58K or other proteins to LEs. Demonstrating the underlying mechanisms awaits further investigation. Nevertheless, these observations may provide an opportunity to enhance PS-ASO release by modulating PS-ASO interaction with these proteins, especially M6PR, to further improve PS-ASO drug potency.

DATA AVAILABILITY

Research data is available upon request. No data was deposited to databases.

SUPPLEMENTARY DATA

Supplementary Data are available at NAR Online.

ACKNOWLEDGEMENTS

The authors wish to thank Tim Vickers and Frank Bennett for stimulating discussion.

FUNDING

Ionis Pharmaceuticals, Inc. Funding for for open access charge: Ionis Pharmaceuticals.

Conflict of interest statement. All authors are employees and shareholders of Ionis Pharmaceuticals, Inc.

REFERENCES

1. Crooke,S.T., Seth,P.P., Vickers,T.A. and Liang,X.H. (2020) The interaction of phosphorothioate-containing RNA targeted drugs with proteins is a critical determinant of the therapeutic effects of these agents. *J. Am. Chem. Soc.*, **142**, 14754–14771.
2. Crooke,S.T., Witztum,J.L., Bennett,C.F. and Baker,B.F. (2018) RNA-targeted therapeutics. *Cell Metab.*, **27**, 714–739.
3. Bennett,C.F., Baker,B.F., Pham,N., Swayze,E. and Geary,R.S. (2017) Pharmacology of antisense drugs. *Annu. Rev. Pharmacol. Toxicol.*, **57**, 81–105.
4. Crooke,S.T. (2017) Molecular mechanisms of antisense oligonucleotides. *Nucleic Acid Ther.*, **27**, 70–77.
5. Liang,X.H., Nichols,J.G., Hsu,C.W., Vickers,T.A. and Crooke,S.T. (2019) mRNA levels can be reduced by antisense oligonucleotides via no-go decay pathway. *Nucleic Acids Res.*, **47**, 6900–6916.
6. Crooke,S.T., Vickers,T.A. and Liang,X.H. (2020) Phosphorothioate modified oligonucleotide-protein interactions. *Nucleic Acids Res.*, **48**, 5235–5253.
7. Liang,X.H., Sun,H., Nichols,J.G. and Crooke,S.T. (2017) RNase H1-dependent antisense oligonucleotides are robustly active in directing RNA cleavage in both the cytoplasm and the nucleus. *Mol. Ther.*, **25**, 2075–2092.
8. Juliano,R.L. (2018) Intracellular trafficking and endosomal release of oligonucleotides: what we know and what we don't. *Nucleic Acid Ther.*, **28**, 166–177.
9. Prakash,T.P., Graham,M.J., Yu,J., Carty,R., Low,A., Chappell,A., Schmidt,K., Zhao,C., Aghajan,M., Murray,H.F. *et al.* (2014) Targeted delivery of antisense oligonucleotides to hepatocytes using triantennary N-acetyl galactosamine improves potency 10-fold in mice. *Nucleic Acids Res.*, **42**, 8796–8807.
10. Wang,S., Allen,N., Vickers,T.A., Revenko,A.S., Sun,H., Liang,X.H. and Crooke,S.T. (2018) Cellular uptake mediated by epidermal growth factor receptor facilitates the intracellular activity of phosphorothioate-modified antisense oligonucleotides. *Nucleic Acids Res.*, **46**, 3579–3594.
11. Crooke,S.T., Wang,S., Vickers,T.A., Shen,W. and Liang,X.H. (2017) Cellular uptake and trafficking of antisense oligonucleotides. *Nat. Biotechnol.*, **35**, 230–237.
12. Miller,C.M., Donner,A.J., Blank,E.E., Egger,A.W., Kellar,B.M., Ostergaard,M.E., Seth,P.P. and Harris,E.N. (2016) Stabilin-1 and Stabilin-2 are specific receptors for the cellular internalization of phosphorothioate-modified antisense oligonucleotides (ASOs) in the liver. *Nucleic Acids Res.*, **44**, 2782–2794.
13. Wang,S., Sun,H., Tanowitz,M., Liang,X.H. and Crooke,S.T. (2016) Annexin A2 facilitates endocytic trafficking of antisense oligonucleotides. *Nucleic Acids Res.*, **44**, 7314–7330.
14. Liang,X.H., Sun,H., Nichols,J.G., Allen,N., Wang,S., Vickers,T.A., Shen,W., Hsu,C.W. and Crooke,S.T. (2018) COPII vesicles can affect

the activity of antisense oligonucleotides by facilitating the release of oligonucleotides from endocytic pathways. *Nucleic Acids Res.*, **46**, 10225–10245.
15. Koller,E., Vincent,T.M., Chappell,A., De,S., Manoharan,M. and Bennett,C.F. (2011) Mechanisms of single-stranded phosphorothioate modified antisense oligonucleotide accumulation in hepatocytes. *Nucleic Acids Res.*, **39**, 4795–4807.
16. Juliano,R.L. (2016) The delivery of therapeutic oligonucleotides. *Nucleic Acids Res.*, **44**, 6518–6548.
17. Wang,S., Sun,H., Tanowitz,M., Liang,X.H. and Crooke,S.T. (2017) Intra-endosomal trafficking mediated by lysobisphosphatidic acid contributes to intracellular release of phosphorothioate-modified antisense oligonucleotides. *Nucleic Acids Res.*, **45**, 5309–5322.
18. Buntz,A., Killian,T., Schmid,D., Seul,H., Brinkmann,U., Ravn,J., Lindholm,M., Knoetgen,H., Haucke,V. and Mundigl,O. (2019) Quantitative fluorescence imaging determines the absolute number of locked nucleic acid oligonucleotides needed for suppression of target gene expression. *Nucleic Acids Res.*, **47**, 953–969.
19. Liang,X.H., Sun,H., Shen,W. and Crooke,S.T. (2015) Identification and characterization of intracellular proteins that bind oligonucleotides with phosphorothioate linkages. *Nucleic Acids Res.*, **43**, 2927–2945.
20. Liang,X.H., Sun,H., Hsu,C.W., Nichols,J.G., Vickers,T.A., De Hoyos,C.L. and Crooke,S.T. (2020) Golgi-endosome transport mediated by M6PR facilitates release of antisense oligonucleotides from endosomes. *Nucleic Acids Res.*, **48**, 1372–1391.
21. Juliano,R.L. and Carver,K. (2015) Cellular uptake and intracellular trafficking of oligonucleotides. *Adv. Drug. Deliv. Rev.*, **87**, 35–45.
22. Zanetti,G., Pahuja,K.B., Studer,S., Shim,S. and Schekman,R. (2011) COPII and the regulation of protein sorting in mammals. *Nat. Cell Biol.*, **14**, 20–28.
23. Pfeffer,S.R. (2009) Multiple routes of protein transport from endosomes to the trans Golgi network. *FEBS Lett.*, **583**, 3811–3816.
24. Brown,F.C., Schindelhaim,C.H. and Pfeffer,S.R. (2011) GCC185 plays independent roles in Golgi structure maintenance and AP-1-mediated vesicle tethering. *J. Cell Biol.*, **194**, 779–787.
25. Liang,X.H., Nichols,J.G., Hsu,C.W. and Crooke,S.T. (2021) Hsc70 facilitates mannose-6-pphosphate receptor-mediated intracellular trafficking and enhances endosomal release of phosphorothioate-modified antisense oligonucleotides. *Nucleic Acid Ther.*, https://doi.org/10.1089/nat.2020.0920.
26. Liang,X.H., Hart,C.E. and Crooke,S.T. (2013) Transfection of siRNAs can alter miRNA levels and trigger non-specific protein degradation in mammalian cells. *Biochim. Biophys. Acta*, **1829**, 455–468.
27. Liang,X.H., Shen,W., Sun,H., Prakash,T.P. and Crooke,S.T. (2014) TCP1 complex proteins interact with phosphorothioate oligonucleotides and can co-localize in oligonucleotide-induced nuclear bodies in mammalian cells. *Nucleic Acids Res.*, **42**, 7819–7832.
28. Schindelin,J., Arganda-Carreras,I., Frise,E., Kaynig,V., Longair,M., Pietzsch,T., Preibisch,S., Rueden,C., Saalfeld,S., Schmid,B. *et al.* (2012) Fiji: an open-source platform for biological-image analysis. *Nat. Methods*, **9**, 676–682.
29. Dunn,K.W., Kamocka,M.M. and McDonald,J.H. (2011) A practical guide to evaluating colocalization in biological microscopy. *Am. J. Physiol. Cell Physiol.*, **300**, C723–C742.
30. Bashour,A.M. and Bloom,G.S. (1998) 58K, a microtubule-binding Golgi protein, is a formiminotransferase cyclodeaminase. *J. Biol. Chem.*, **273**, 19612–19617.
31. Gao,Y. and Sztul,E. (2001) A novel interaction of the Golgi complex with the vimentin intermediate filament cytoskeleton. *J. Cell Biol.*, **152**, 877–894.
32. Zuber,C., Spiro,M.J., Guhl,B., Spiro,R.G. and Roth,J. (2000) Golgi apparatus immunolocalization of endomannosidase suggests post-endoplasmic reticulum glucose trimming: implications for quality control. *Mol. Biol. Cell*, **11**, 4227–4240.
33. Strating,J.R. and Martens,G.J. (2009) The p24 family and selective transport processes at the ER-Golgi interface. *Biol. Cell*, **101**, 495–509.
34. Lima,W.F., Murray,H.M., Damle,S.S., Hart,C.E., Hung,G., De Hoyos,C.L., Liang,X.H. and Crooke,S.T. (2016) Viable RNaseH1 knockout mice show RNaseH1 is essential for R loop processing, mitochondrial and liver function. *Nucleic Acids Res.*, **44**, 5299–5312.
35. Lieu,Z.Z., Derby,M.C., Teasdale,R.D., Hart,C., Gunn,P. and Gleeson,P.A. (2007) The golgin GCC88 is required for efficient retrograde transport of cargo from the early endosomes to the trans-Golgi network. *Mol. Biol. Cell*, **18**, 4979–4991.
36. Derby,M.C., Lieu,Z.Z., Brown,D., Stow,J.L., Goud,B. and Gleeson,P.A. (2007) The trans-Golgi network golgin, GCC185, is required for endosome-to-Golgi transport and maintenance of Golgi structure. *Traffic*, **8**, 758–773.
37. Roquemore,E.P. and Banting,G. (1998) Efficient trafficking of TGN38 from the endosome to the trans-Golgi network requires a free hydroxyl group at position 331 in the cytosolic domain. *Mol. Biol. Cell*, **9**, 2125–2144.
38. Banting,G. and Ponnambalam,S. (1997) TGN38 and its orthologues: roles in post-TGN vesicle formation and maintenance of TGN morphology. *Biochim. Biophys. Acta*, **1355**, 209–217.
39. Moremen,K.W. (2002) Golgi alpha-mannosidase II deficiency in vertebrate systems: implications for asparagine-linked oligosaccharide processing in mammals. *Biochim. Biophys. Acta*, **1573**, 225–235.
40. Lin,S.X., Mallet,W.G., Huang,A.Y. and Maxfield,F.R. (2004) Endocytosed cation-independent mannose 6-phosphate receptor traffics via the endocytic recycling compartment en route to the trans-Golgi network and a subpopulation of late endosomes. *Mol. Biol. Cell*, **15**, 721–733.
41. Shen,W., Liang,X.H. and Crooke,S.T. (2014) Phosphorothioate oligonucleotides can displace NEAT1 RNA and form nuclear paraspeckle-like structures. *Nucleic Acids Res.*, **42**, 8648–8662.
42. Tanowitz,M., Hettrick,L., Revenko,A., Kinberger,G.A., Prakash,T.P. and Seth,P.P. (2017) Asialoglycoprotein receptor 1 mediates productive uptake of N-acetylgalactosamine-conjugated and unconjugated phosphorothioate antisense oligonucleotides into liver hepatocytes. *Nucleic Acids Res.*, **45**, 12388–12400.
43. Nonnenmacher,M.E., Cintrat,J.C., Gillet,D. and Weber,T. (2015) Syntaxin 5-dependent retrograde transport to the trans-Golgi network is required for adeno-associated virus transduction. *J. Virol.*, **89**, 1673–1687.
44. Sandvig,K., Skotland,T., van Deurs,B. and Klokk,T.I. (2013) Retrograde transport of protein toxins through the Golgi apparatus. *Histochem. Cell Biol.*, **140**, 317–326.
45. Linders,P.T., Horst,C.V., Beest,M.T. and van den Bogaart,G. (2019) Stx5-mediated ER-Golgi transport in mammals and yeast. *Cells*, **8**, 780.
46. Hennig,D., Scales,S.J., Moreau,A., Murley,L.L., De Mey,J. and Kreis,T.E. (1998) A formiminotransferase cyclodeaminase isoform is localized to the Golgi complex and can mediate interaction of trans-Golgi network-derived vesicles with microtubules. *J. Biol. Chem.*, **273**, 19602–19611.
47. Bloom,G.S. and Brashear,T.A. (1989) A novel 58-kDa protein associates with the Golgi apparatus and microtubules. *J. Biol. Chem.*, **264**, 16083–16092.
48. Vickers,T.A. and Crooke,S.T. (2014) Antisense oligonucleotides capable of promoting specific target mRNA reduction via competing RNase H1-dependent and independent mechanisms. *PLoS One*, **9**, e108625.
49. Liang,X.H., De Hoyos,C.L., Shen,W., Zhang,L., Fazio,M. and Crooke,S.T. (2021) Solid-phase separation of toxic phosphorothioate antisense oligonucleotide-protein nucleolar aggregates is cytoprotective. *Nucleic Acid Ther.*, **31**, 126–144.